Systems & Control Transactions

Research Article
Foundations of Computer Aided Process Design (FOCAPD 2024)
Breckenridge, Colorado, USA. July 14-18, 2024
Peer Reviewed Conference Proceeding

PSE PRESS

Optimization of Solid Oxide Electrolysis Cell Systems Accounting for Long-Term Performance and Health Degradation

Nishant V. Giridhar[a], Debangsu Bhattacharyya[a]*, Douglas A. Allan[b], Stephen E. Zitney[c], Mingrui Li[d], Lorenz T. Biegler[d]

[a] Department of Chemical and Biomedical Engineering, West Virginia University, Morgantown, WV 26506, USA
[b] NETL Support Contractor, Pittsburgh, PA 15236, USA
[c] National Energy Technology Laboratory, Morgantown, WV 26507, USA
[d] Department of Chemical Engineering, Carnegie Mellon University, Pittsburgh, PA 15213, USA
* Corresponding Author: debangsu.bhattacharyya@mail.wvu.edu

ABSTRACT

This study focuses on optimizing solid oxide electrolysis cell (SOEC) systems for efficient and durable long-term hydrogen (H_2) production. While the elevated operating temperatures of SOECs offer advantages in terms of efficiency, they also lead to chemical degradation, which shortens cell lifespan. To address this challenge, dynamic degradation models are coupled with a steady-state, two-dimensional, non-isothermal SOEC model and steady-state auxiliary balance of plant equipment models, within the IDAES modeling and optimization framework. A quasi-steady state approach is presented to reduce model size and computational complexity. Long-term dynamic simulations at constant H_2 production rate illustrate the thermal effects of chemical degradation. Dynamic optimization is used to minimize the lifetime cost of H_2 production, accounting for SOEC replacement, operating, and energy expenses. Several optimized operating profiles are compared by calculating the Levelized Cost of Hydrogen (LCOH).

Keywords: Fuel Cells, Dynamic Degradation Modelling, Hydrogen, Optimization, Solid Oxide Cells

INTRODUCTION

Solid oxide cells (SOCs) are flexible energy conversion and H_2 generation devices that have many benefits including modularity, high theoretical efficiency, and low operating greenhouse gas emissions. They can be operated reversibly in either power generation mode as a solid oxide fuel cell (SOFC) or H_2 production mode as a solid oxide electrolysis cell (SOEC). Steam electrolysis in SOECs has a variety of benefits over a conventional steam-methane reforming process such as no direct emission of CO_2 when renewable sources of electricity are used. High-temperature SOCs offer high electrical efficiency especially at high temperatures.

However, the high temperature needed for achieving high efficiency in SOCs also leads to chemical degradation of the microstructure in the electrodes and electrolytes. Chemical degradation results in changes in the composition and microstructure of the triple-phase boundary. The dynamics of these changes are very slow, but the changes can steadily build up during the operating lifetime of a cell. Chemical degradation causes an increase in the voltage losses that reduce the effective voltage utilized for electrolysis.

V_{cell}, the cell voltage that contributes to electrolysis, is given by Equation 1. In Equation 1, V_{Nernst} is the Nernst potential and V_{act}, V_{Ohmic} , and V_{conc} are the activation, Ohmic, and concentration overpotentials. The magnitudes of these overpotentials depend on the operating conditions of the cell, but these losses are inevitable even in fresh, undegraded cells. The total overpotential due to all long-term chemical degradation mechanisms is given by $V_{degradation}$. In a new (i.e., undegraded) cell, the $V_{degradation}$ term is 0, but this term increases with time.

$$V_{cell} = V_{Nernst} - V_{act} - V_{Ohmic} - V_{degradation} \quad (1)$$

Figure 1 shows a typical SOEC and the reactions

occurring in the fuel and oxygen electrodes. In the oxygen electrode (anode during electrolysis), high partial pressure of oxygen contributes to the oxidation of the active material LSM-YSZ. In the fuel electrode, nickel (Ni) agglomeration occurs due to Ostwald ripening.

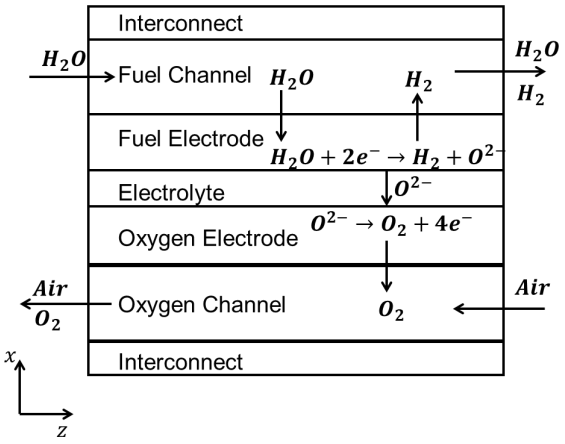

Figure 1. SOEC Schematic and Reactions

In the literature, many approaches have been proposed to include degradation models for making SOC design and operation decisions. A few relevant optimization studies are reviewed here. For detailed review, we refer readers to [1]. Parhizkar et al. [2] combined microstructure degradation models with a simplified input-output SOFC performance model to perform steady-state optimization to identify operating conditions for minimizing the cost of electricity. Naeini et al. [3] coupled a data-driven model for SOEC degradation with a steady-state model for SOEC operation. In their work, the Levelized Cost of Hydrogen (LCOH) is minimized over a 20-year operating horizon.

In this work, models of key degradation mechanisms are coupled with a first principles two-dimensional (2D) non-isothermal SOEC model. This work seeks to fill two gaps in the existing literature. First, most modeling studies in the literature use isothermal 0D models; therefore, spatial variation and thermal characteristics of a degraded cell are neglected. The 2D non-isothermal SOC model used in this work provides detailed insights into the spatial distribution of degradation in each cell. A second gap, which this work aims to fill, is that most SOC degradation simulation studies do not consider the effects of degradation on the balance of plant. While some studies incorporate simplified heating and compression duties in their calculations for total energy consumption, this work extends this to capture the impact of cell level degradation on the balance of plant by considering a fully modeled SOEC flowsheet. The flowsheet model is used in dynamic optimization to identify optimal operating profiles for system- and cell-level decision variables as a function of time.

MODELING AND METHODS

Flowsheet modeling details

As shown in Figure 2, the SOEC hydrogen production system is modeled as a collection of linked unit models in the open-source IDAES, equation-oriented IDEAS (Institute for the Design of Advanced Energy Systems) platform. The system consists of an SOEC stack (modeled as a single cell), and electric heaters for the feed and sweep input streams along with heat exchangers for heat recovery. For a detailed description of SOEC flowsheet modeling details, we refer readers to [4-5]. The models used in this study are available in the open-source IDAES modeling framework [9].

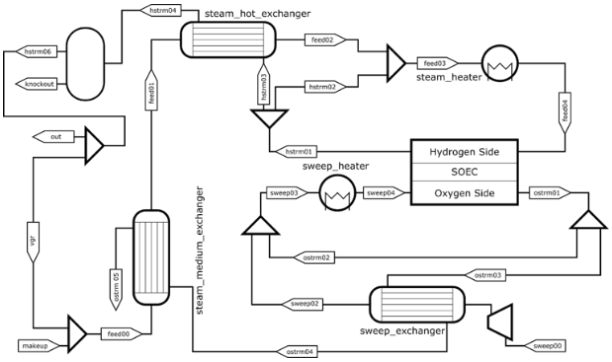

Figure 2. SOEC system flowsheet

Health modeling

Degradation mechanisms in SOCs vary depending on the materials of construction of the cell. For this study, we consider fuel electrode of a Ni-YSZ composite, an oxygen electrode of LSM-YSZ separated by a YSZ electrolyte as a part of a planar fuel electrode supported SOC.

One of the dominant degradation mechanisms that take place in the fuel electrode is the agglomeration of Ni particles due to surface diffusion. The dynamics of the Ni particle growth are described by Equation 2 [6]. Here, $\bar{d}_{Ni}$ is the average Ni particle diameter, $m = 0.5$ and $n = 8$.

$$\frac{d(\bar{d}_{Ni})}{dt} = \frac{a'}{d_{Ni}^{n-1}} \left(\frac{P_{H_2O}}{P_{H_2}^{0.5}} \right)^m e^{\frac{-E_a}{RT}} \quad (2)$$

The oxygen electrode undergoes degradation due to the growth of oxide scales under high oxygen partial pressure. Under these conditions, Wagner's law for parabolic oxidation is used as a semi-empirical model to describe growth of oxide scale. In LSM-YSZ electrodes, the scales formed are of lanthanum zirconate (LZO) and chromium oxide (COS). The chromium oxide scale is localized to the interface between the oxygen electrode and interconnect. Equation (3) describes the temperature-dependent Wagner's law for a general oxide scale growth length l_{sc} [7]. Here, $X_{0,sc}$, ρ_{sc}, K_{sc}, and E_{sc} are the weight fraction, density, weight gain rate, and activation

energies of oxide scale growth, respectively.

$$\frac{dl_{sc}}{dt} = \frac{K_{sc}}{2\left(X_{0,sc}\rho_{sc}\right)^2 l_{sc}} e^{-\frac{E_{sc}}{RT}} \quad \forall \; sc \in \{COS, LZO\} \qquad (3)$$

Other degradation mechanisms that are modeled include coarsening of the LSM-YSZ oxygen electrode and phase transformation of the YSZ electrolyte. Additionally, we make use of property models to relate microstructure parameters to degradation overpotentials [8].

Solution methodology

Incorporating degradation models into first principles unit models requires solving a differential algebraic equation (DAE) system with multiple timescales. For the SOEC system, these timescales can be broadly divided into two categories: one faster timescale for process operations and SOEC dynamics (minutes to hours) and another slower timescale for degradation (hundreds of hours). To simplify the problem, we assume quasi-steady state for the faster timescale processes. This allows us to discretize and dynamically integrate the slower degradation timescale. With this approach, we can simulate SOEC operation with degradation effects for extended periods, spanning tens of thousands of operational hours, providing insights into long-term performance and design strategies.

We employ the implicit Euler method to discretize the degradation dynamic equations. The discretized system of equations can be solved simultaneously and efficiently using a nonlinear solver such as IPOPT [10]. Because of the quasi-steady state assumption, the only active differential equations in the model are those pertaining to the slow degradation dynamics. The advantage of a simultaneous solution method is the ability to optimize across the entire operational horizon, ensuring a comprehensive assessment of system performance. Additionally, this approach enables the incorporation of constraints spanning multiple time points, thus providing enhanced modeling versatility. In contrast, the sequential time-stepping approach restricts optimization to instantaneous performance metrics like instantaneous efficiency.

Hydrogen Production Profiles

The discretized SOEC system model is used to assess different long-term operating scenarios by first specifying the nature of the hydrogen production profile.

Constant H_2 Production: In this profile, a constant H_2 production rate is maintained throughout the operating lifetime. As shown in Equation 4, an equality constraint indexed over time ensures that the average current density J_{avg} remains constant. Here, $j_{t,z}$ is the local current density at a point z along the length of the cell and N_z is the number of finite elements. As degradation proceeds, it is expected that increased degradation losses will result in an increase in operating voltage to sustain the fixed H_2 production rate.

$$\frac{1}{N_z}\sum_{z} j_{t,z} = J_{avg,0} \qquad \forall \quad t \qquad (4)$$

Constant Potential Operation: In this strategy, a constant cell potential is maintained over time [3]. This keeps cell-level energy consumption constant. However, as degradation progresses, current density decreases. This leads to a gradual reduction in H_2 production at a constant operating temperature. However, by varying the cell operating temperature over time, more complex operating scenarios can be investigated. Cell voltage is held constant by fixing operating voltage for all time points (Equation 5).

$$V_{cell,t} = V_{cell,0} \qquad \forall \quad t \qquad (5)$$

Dynamic optimization

Typically, steady-state optimization is used to determine the operational setpoints of a system. In this case, minimization of the system power requirement for a given H_2 production rate [5]. This methodology can be used to determine steady-state optimal operating conditions corresponding to different load conditions. In the absence of degradation, operational efficiency, power consumption, and local cell temperature profile would remain at the steady-state optimal value. In this work, we provide a methodology to optimize the operational profile over 20,000 hours for long-term stability and efficient operation, while accounting for performance degradation.

For long-term dynamic optimization, we propose to maximize the integral average efficiency over the operating lifetime (Equation 6). As a surrogate for system efficiency, we use a simplified version as described in [11]. Under constant H_2 load, the numerator is invariant, and the objective simplifies to the minimization of system power consumption. Obviously, under constant potential operation, the numerator is not constant. Here, P_{system} is the total electric power consumption of the system, including stack work, electric heater, and blower duties (Equation 7).

$$\max \sum_{t \in time} \frac{HHV\left(\dot{m}_{H_2,t}\right)}{P_{system,t}} \qquad (6)$$

$$P_{system} = P_{SOEC} + P_{sweep\ heater} + P_{feed\ heater} + P_{blower} \qquad (7)$$

A second operational strategy involves minimization of the degradation rate. To include all degradation effects into one combined term, it is desirable to use the degradation overpotential $V_{degradation}$ in Equation 1. However, since the overpotential at any given point in time

Table 1: Summary of Optimization Results

H_2 Production Profile	Objective Function	Avg. H_2 Production Rate ($\times 10^7 kg/yr$)	Sp. Energy Consumption (kWh/ kg H_2)	Voltage Degradation Rate (%/ khr)	Replacement Time (years)	LCOH ($ /kWh)
Constant H_2 Production Rate	Maximize Integral Efficiency	4.74	36.6	4.4	1.5	0.31
	Minimize Degradation Rate	4.74	40.4	1.5	4.0	0.33
Constant Potential Operation	Maximize Integral Efficiency	3.39	35.6	2.7	2.0	0.29
	Minimize Degradation Rate	1.31	41.7	0.7	8.0	0.37
	Maximize H_2 Production	3.93	38.9	5.0	1.5	0.34

depends on the operating temperature and composition following an Arrhenius-type temperature dependence, we consider the voltage at a reference temperature $\tilde{V}$. This ensures that the voltage degradation rate for optimization only depends on the operating trajectory. With this we minimize the average voltage degradation rate from t=0 to t=t_f, the final time point (Equation 8).

$$\min \frac{\tilde{V}_{t_f} - \tilde{V}_0}{\tilde{V}_0} \tag{8}$$

Finally, under constant potential operation, market conditions may require the system to operate at the highest possible H_2 production rate ($\dot{m}_{H_2}$). This can be achieved by maximizing the H_2 production rate (Equation 9).

$$\max \sum_{t \in time} \dot{m}_{H_2,t} \, \Delta t \tag{9}$$

The decision variables for optimization include feed and trim heater duties, recycle ratios, blower flowrate, sweep and steam inlet and outlet temperatures. For details on bounds and operational constraints refer to [5].

Levelized Cost of H_2 (LCOH) Calculation

The different optimized cases are compared based on the resultant LCOH, as shown in Equation 10. We compute the LCOH by modifying the method of [12] to incorporate stack replacement costs. The LCOH includes the capital recovery factor (CRF) and capital costs (CC) for the stack and balance of the plant (BOP). $OC, EC,$ and $m_{H_2,\text{ lifetime}}$ are the operating costs, energy costs, and lifetime H_2 production, respectively. Costing parameters are obtained from [12].

$$LCOH = \frac{CRF_{BOP} CC_{BOP} + \sum_{i=1}^{R} CRF_{\text{stack},i} CC_{\text{stack}} + OC + EC}{m_{H_2,\text{ lifetime}}} \tag{10}$$

The number of stack replacements (n_{rep}) over the plant lifetime of 30 years is computed based on the extent of degradation at the end of the 20,000-hour optimization horizon as per Equations 11 and 12.

$$\text{Replacement time} = \frac{\Delta \tilde{V}_{limit}}{\left(\frac{\Delta \tilde{V}}{\Delta t}\right)_{avg}} \tag{11}$$

$$n_{rep} = \frac{30 \text{ years}}{\text{replacement time}} \tag{12}$$

RESULTS

Figure 3 compares 20,000 hours of operation, at constant current density and constant potential through simulations. As the degradation overpotential increases over time, we observe that constant current density operation results in a higher voltage degradation rate than constant potential operation. Due to the increase in Ohmic resistance, the thermal characteristics along the length of the cell change with time.

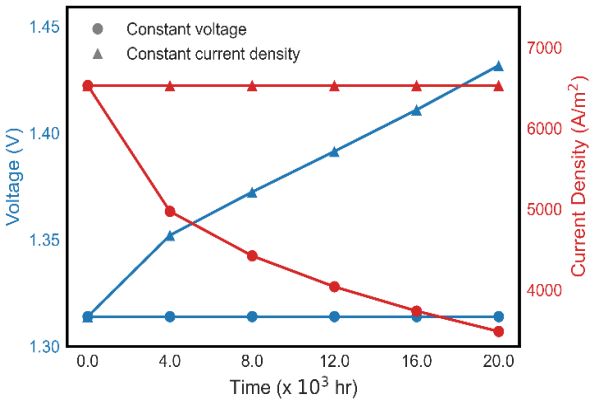

Figure 3. Effect of degradation on voltage and current density

As shown in Figure 4, there is a significant increase in the average temperature along the length of the cell for constant current density operation. Here the inlet temperatures were held constant over the 20,000 hours

of operation.

The spatial temperature profile shown is at the center of the cell along the electrolyte layer. During constant current density operation, we observe a large increase in local cell temperature. The increase in degradation overpotential results in an increase in operating potential, which corresponds to operation above the thermoneutral voltage. Furthermore, the larger Ohmic resistance due to degradation also results in higher Ohmic heating. Under constant potential operation, a drop in current density results in lower cell temperatures.

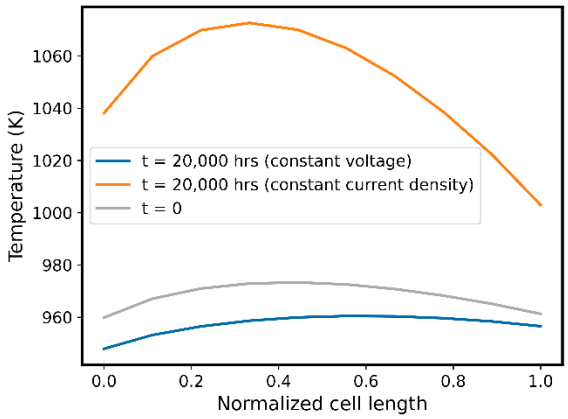

Figure 4. Change in temperature profile due to degradation

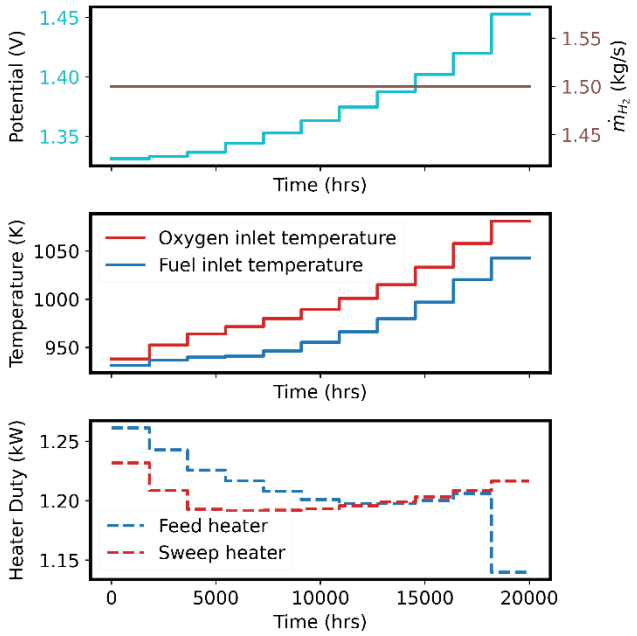

Figure 5. Optimal Constant H_2 Production Operation (Maximize Integral Efficiency)

Table 1 compares key performance measures from the different dynamic optimization case studies. These include the average H_2 production rate, specific energy consumption, and average degradation rate as calculated in Equation 13.

$$\text{Voltage Degradation Rate} = \frac{1}{t_f}\frac{\tilde{V}_t - \tilde{V}_0}{\tilde{V}_0} \times 100 \qquad (13)$$

The initial operating point for all cases is identical, and the specific operating conditions were obtained by a steady-state optimization to ensure a H_2 production rate of 1.5 kg/s. This corresponded to an optimal initial voltage of 1.31 V. For more details on the steady-state optimization, refer to [5].

When operating at a constant H_2 production rate, the choice of operating objective can result in significant changes in specific energy consumption and degradation. In this work, we consider the fixed H_2 production rate achieved by constant current density operation to be the upper limit of H_2 production by the system. Based on the costing methods used in this study, a lower LCOH is obtained when integral system efficiency is maximized. Figure 5 describes the temporal profiles of the key decision variables to achieve the maximum integral efficiency. Due to increased voltage losses caused by degradation, operating potential must be increased to maintain the initial H_2 production rate ($\dot{m}_{H_2}$) of 1.5 kg/s. Since inevitable losses depend directly on temperature, the optimal inlet temperatures for both the fuel and oxygen electrodes must be increased to maintain voltage efficiency. Feed and sweep heater duties are kept low due to the presence of recycle streams. Therefore, internal stack resistive heating is used instead of electric heating in the trim heaters. In contrast, degradation rate can be minimized by operating the cell at low temperatures. This results in a significant increase in inevitable losses and, consequently, there is a drop in efficiency as evidenced by the increase in specific energy consumption.

Under a constant potential operating regime (Figure 6), it is observed that the degradation rate depends heavily on the specific operating profile even when operating under constant potential. Under a constant potential over the operating lifetime of the cell, the lowest degradation rate is achieved by operating the cell at low temperatures and, consequently, a very low H_2 production rate (~70% reduction compared to constant H_2 production). Consequently, the specific energy consumption and LCOH when the degradation rate is minimized at constant potential is the highest of all the cases. On the other hand, if operation is optimized for maximum H_2 production under a constant operating potential, we observe a significantly higher degradation rate. At any point in time to maximize H_2 production rate at a constant operating potential, the cell must be operated at the upper bounds of the temperature. Therefore, high temperature ensures a high instantaneous H_2 production rate at all points in time. Consequently, the degradation rate is significantly higher than in all other cases, including those

where H_2 production is held constant.

Figure 6 describes the optimal operating profiles for constant voltage with the objective to maximize integral efficiency. While keeping potential constant, initially it is preferred to operate at a decreasing H_2 production rate to minimize degradation in the early periods of a cells lifetime. Once degradation in the cell reaches a certain level, it is observed that the H_2 production rate increases again. This is likely because of a phenomenon known as cell break in, resulting from the different rates of degradation of the electrode materials. For example, in Ni-YSZ fuel electrodes, there is a coarsening of Ni particles, while the YSZ particles remain unchanged. The YSZ backbone therefore has a limiting effect on the maximal extent of Ni degradation. Similarly, the parabolic growth rate of oxide scales in the oxygen electrode decreases with the increase in the extent of the oxide scale. To evaluate all optimization formulations and H_2 demand profiles, the LCOH was computed for the five cases. For details on LCOH calculations and costing methodology, refer to [12]. Results presented in the paper correspond to an electricity price of 0.30 $/kWh. According to this costing methodology, operating at a constant potential and maximizing integral average efficiency leads to the lowest LCOH. The cases with the highest LCOH are those with high energy consumption, where the degradation rate is explicitly minimized. This indicates that system efficiency and H_2 production rate have a higher impact on LCOH than stack replacement costs.

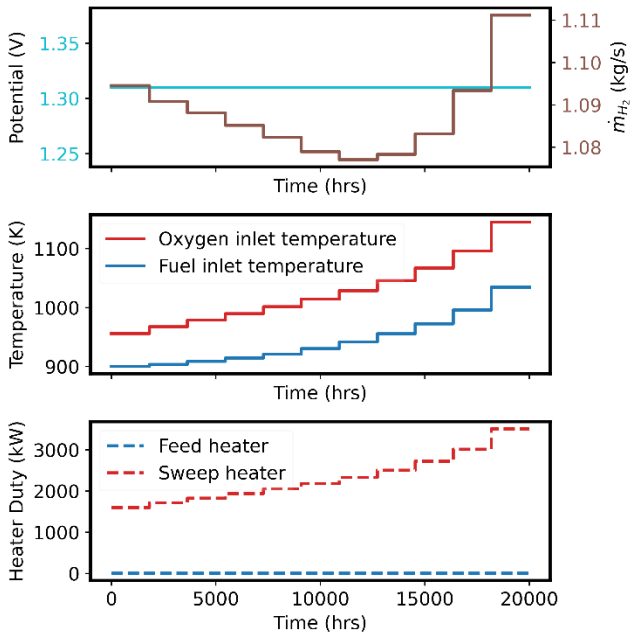

Figure 6. Optimal Constant Voltage Operation (Maximize Integral Efficiency)

CONCLUSION

In this work, we present a dynamic optimization methodology to obtain time dependent operating points for an SOEC system considering the effects of chemical degradation on operating efficiency. The quasi-steady state assumption enables model size reduction to perform dynamic optimization on a fully discretized DAE model.

The 2D non-isothermal SOEC model used in this study captures the thermal implications of chemical degradation. In addition to an increase in electrochemical losses, it is found that chemical degradation results in an overall increase in exothermicity due to an increase in resistive heating. The balance-of-plant model facilitates accurate estimation of SOEC system energy requirements from auxiliary equipment such as heaters and blowers.

Dynamic optimization of long-term operating conditions over 20,000 hours was performed under two H_2 production profiles; namely, constant H_2 production and constant potential operation. This study shows that both operating profiles can result in efficient long-term operation depending on the optimization objective. Strong trade-offs between the integral average operating efficiency and the degradation rate are observed. LCOH is computed for each of the cases and is used to evaluate the different operating trajectories. Operating at a constant potential while maximizing the integral efficiency is found to have the lowest LCOH at 0.29 $/kWh H_2 with a replacement schedule of 2 years. It must be noted that the LCOH calculation depends on many factors such as the interaction between stack replacement costs and the price of electricity. In a situation where stack replacement costs are higher, it is possible that lower degradation rates would be favorable. Furthermore, this study does not consider the impact of operation on physical degradation. This poses the challenge of incorporating operating profiles from a shorter timescale of daily operation.

ACKNOWLEDGEMENTS

This work was conducted as part of the Institute for the Design of Advanced Energy Systems (IDAES) with support from the U.S. Department of Energy's Office of Fossil Energy and Carbon Management through the Simulation-based Engineering Research Program.

This project was funded by the Department of Energy, National Energy Technology Laboratory an agency of the United States Government, through a support contract. Neither the United States Government nor any agency thereof, nor any of its employees, nor the support contractor, nor any of their employees, makes any warranty, expressor implied, or assumes any legal liability or responsibility for the accuracy, completeness, or usefulness of any information, apparatus, product, or process

disclosed, or represents that its use would not infringe privately owned rights. Reference herein to any specific commercial product, process, or service by trade name, trademark, manufacturer, or otherwise does not necessarily constitute or imply its endorsement, recommendation, or favoring by the United States Government or any agency thereof. The views and opinions of authors expressed herein do not necessarily state or reflect those of the United States Government or any agency thereof.

REFERENCES

1. Peng, J., Zhao, D., Xu, Y., Wu, X., & Li, X. Comprehensive analysis of solid oxide fuel cell performance degradation mechanism, prediction, and optimization studies. Energies, 16(2), 788 (2023).
2. Parhizkar, T, and Roshandel, R. Long term performance degradation analysis and optimization of anode supported solid oxide fuel cell stacks. *Energy conversion and management* 133: 20-30 (2017).
3. Naeini, M., Cotton, J. S., & Adams, T. A. An eco-technoeconomic analysis of hydrogen production using solid oxide electrolysis cells that accounts for long-term degradation. *Frontiers in Energy Research* 10, 1015465 (2022).
4. Bhattacharyya, D., Rengaswamy, R., & Finnerty, C. Dynamic modeling and validation studies of a tubular solid oxide fuel cell. *Chemical Engineering Science*, 64(9), 2158-2172 (2009).
5. Allan, D.A., Dabadghao, V., Li, M., Eslicka, J.C., Ma, J., Bhattacharyya, D., Zitney, S.E. and Biegler, L.T. NMPC for Setpoint Tracking Operation of a Solid Oxide Electrolysis Cell System. National Energy Technology Laboratory (NETL), Pittsburgh, PA, Morgantown, WV, and Albany, OR (United States) (2023).
6. Sehested, J., Gelten, J. A., & Helveg, S. Sintering of nickel catalysts: Effects of time, atmosphere, temperature, nickel-carrier interactions, and dopants. *Applied Catalysis A: General*, 309(2), 237-246 (2006).
7. Kamkeng, A. D., & Wang, M. Long-term performance prediction of solid oxide electrolysis cell (SOEC) for CO2/H2O co-electrolysis considering structural degradation through modelling and simulation. *Chemical Engineering Journal*, 429, 132158 (2022).
8. Mason, J., Celik, I., Lee, S., Abernathy, H., & Hackett, G. Performance degradation predictions based on microstructural evolution due to grain coarsening effects in solid oxide fuel cell electrodes. *Journal of The Electrochemical Society*, 165(2), F64 (2018).
9. Lee A., Ghouse JH, Eslick JE, et al., The IDAES process modeling framework and model library—Flexibility for process simulation and optimization. *J Adv Manuf Process* 3(3): e10095 (2021)
10. Wächter, A., & Biegler, L. T. On the implementation of an interior-point filter line-search algorithm for large-scale nonlinear programming. *Mathematical programming*, 106, 25-57 (2006).
11. Harrison, K. W., Remick, R., Hoskin, A., & Martin, G. D. Hydrogen production: fundamentals and case study summaries (No. NREL/CP-550-47302). National Renewable Energy Lab.(NREL), Golden, CO (United States) (2010).
12. Eslick, J., Noring, A., Susarla, N., Okoli, C., Allan, D., Wang, M., ... & Burgard, A. Technoeconomic Evaluation of Solid Oxide Fuel Cell Hydrogen-Electricity Co-Generation Concepts (No. DOE/NETL-2023/4322). National Energy Technology Laboratory (NETL), Pittsburgh, PA, Morgantown, WV, and Albany, OR (United States) (2023).